Magnetoresistance fluctuations in a weak disorder indium nitride nanowire

Y W Su[1,7,8], K Aravind[2,7,8], C S Wu[3], Watson Kuo[4], K H Chen[5],
L C Chen[6] and K S Chang-Liao[2], W F Su[1] and C DChen[7,9]

[1] Department of Materials Science and Engineering, National Taiwan University, Taipei 106, Taiwan

[2] Department of Engineering and System Science, National Tsing Hua University, Hsinchu 300, Taiwan

[3] Department of Physics, National Chang-Hua University of Education, ChangHua 500, Taiwan

[4] Department of Physics, National Chung Hsing University, Taichung 402, Taiwan

[5] Institute of Atomic and Molecular Sciences, Academia Sinica, Taipei 106, Taiwan

[6] Center for Condensed Matter Sciences, National Taiwan University, Taipei 106, Taiwan

[7] Institute of Physics, Academia Sinica, Nankang 115, Taipei, Taiwan

E-mail: chiidong@phys.sinica.edu.tw

Abstract

We report measurements of magnetoresistance (MR) fluctuations in a weak disorder indium
nitride nanowire. The MR fluctuations are reproducible, aperiodic and symmetric in magnetic
field but are asymmetric upon reversal of bias direction. The fluctuations are analysed for both
perpendicular and parallel external magnetic field configurations in the light of tunnel
magnetoresistance at low field and impurity scattering at higher field. The asymmetry in bias
reversal is caused by breakdown of time reversal symmetry.

(Some figures in this article are in colour only in the electronic version)

Nanowires are a promising class of powerful materials, which, together with controlled growth and organization, can open avenues for next generation nano-scale electronic devices [1]. Indium nitride (InN) is an interesting candidate for these applications because of its revised direct band gap of 0.7–0.8 eV in the visible range [2–4]. Magnetoresistance (MR) is the relative change in electrical resistance upon application of a magnetic field and this has already found much scope for application. It is our attempt to integrate these versatile nanowire materials with advanced fabrication technology. The state-of-the-art patterning techniques allow us to make electrodes with very small separation so that the device falls into the mesoscopic regime. In this paper we present the interesting interplay between MR fingerprints and diffusive electron transport in single crystal wurtzite InN nanowires in both parallel and perpendicular magnetic field configurations. In particular, the low field (within ± 1 kGs) data show typical signatures of tunnel magnetoresistance (TMR) while the high field (up to ± 50 kGs) data exhibit aperiodic, non-attenuating fluctuations, which are a characteristic manifestation of the

hypothesis [5] predicting a complete change in impurity configuration in a sweeping magnetic field.

Single crystalline nanowires used in this device were grown by guided stream thermal chemical vapour deposition with trimethyl indium as indium source, ammonia as nitrogen source and gold as catalyst [6]. The diameters of the wires were in the range 35–120 nm with a typical length 15–20 μm. The nanowires were first dispersed in isopropanol solution. A few droplets of this solution were then placed on Si substrates with micrometre-sized Pt/Ti measurement pads pre-fabricated on a 300 nm thick SiO_2 oxide surface. Subsequently, nano-scaled electrodes were fabricated by standard electron beam lithographic technology, which served as inter-connectors between nanowires and Pt/Ti pads. Electron beam writing and identification of the positions of the dispersed nanowires for e-beam exposure purpose were performed using a field emission scanning electron microscope (FESEM). The nanometre electrodes were made of Ni (50 nm) covered with Au (50 nm) protection layer and were found to provide good Ohmic contacts to the InN nanowires. The top-left inset of figure 1 shows an FESEM image of the measured device. For this device the wire diameter is about 80 nm and the separation between the source and drain electrodes is approximately

[8] These authors contributed equally for this work.
[9] Author to whom any correspondence should be addressed.
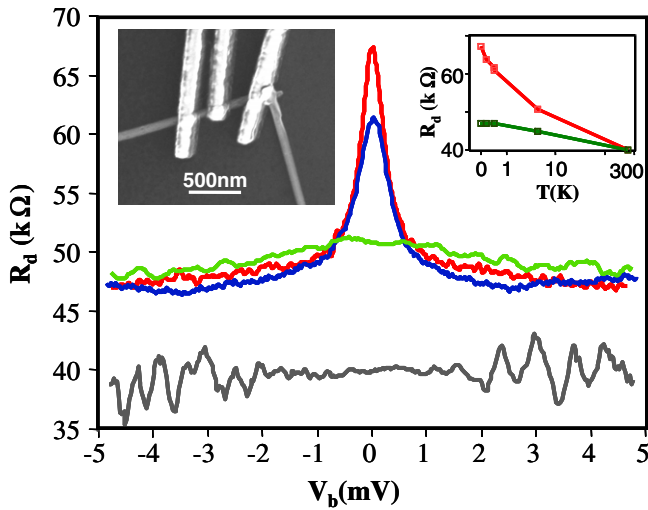
Figure 1. Differential resistance (dV_b/dI) as a function of bias voltage at $T = 300$ K (grey), 4.2 K (green), 0.55 K (blue) and 0.32 K (red). The variation of the differential resistance R_d as a function of temperature is plotted in the top-right inset, the red curve is for the zero bias resistance while the green curve is the asymptotic resistance. The top-left inset is an FESEM image of the nanowire device under study. The left and central electrodes seen in the SEM image are used to study the electron transport and can be labelled as source and drain, respectively, for clarity and convenience in discussions. The right electrode is used to estimate the contact resistances. (Colour online.)

120 nm. The differential resistance measurements were performed using a dc current/voltage amplifier equipped with external bias inputs and two lock-in amplifiers (Signal Recovery 7265) for measuring current and voltage signals simultaneously. The resistance values at bias V_b were obtained by setting an appropriate offset voltage to the external bias input and an excitation of 19.3 μV at 1.7 Hz.

Before discussing the transport characteristics and MR signatures of this device, it is useful to understand the intrinsic electronic properties of InN nanowires. It is widely believed that clean InN surface has electron accumulation [7] unlike other III–V semiconductors because its branch point energy lies within the conduction band at the Γ-point [8]. In InN wires, the presence of nitrogen vacancies, residual hydrogen and other unintentional impurities was reported [9], which is responsible for the appearance of surface charge states, making the wires a weak disorder system. We shall confirm this point using the observed weak localization and MR fluctuations and deduce the phase breaking length.

The FESEM of the measured device is shown in the left inset of figure 1. The main panel shows the variation of differential resistance $R_d \equiv dV_b/dI$ with bias V_b. The IV_b characteristics (not shown) at room temperature are linear with a linear resistance equal to 39 KΩ and as the temperature is lowered to 0.3 K, the IV_b characteristic becomes nonlinear: the current at low bias voltages is suppressed whereas the asymptotic resistance increases slightly to 47 KΩ. This is in contrast to the observed trend of decreasing resistance with decreasing temperature in InN nanowires as reported by Chang *et al* [9] in which the decreased resistance was attributed to thermally induced structural changes while neglecting the

temperature dependence of the contact resistance. In our device, this decreasing part is compensated by the increased contact resistance due to fluctuation-induced tunnelling conduction at the disordered wire–electrode interface [10]. From three-probe measurements, we extracted a contact resistance of around 20 KΩ. This number is in line with other measured devices made with the same technique. Assuming a similar contact resistance for other leads, the wire resistance is estimated to be about 7 KΩ at $T = 0.3$ K. The observed peak in differential resistance $R_d \equiv dV_b/dI$ at zero-bias can be attributed to electron–electron interaction in a disordered nanowire. At low temperatures, the IV_b characteristics can be described by a power-law of a form $I \propto V_b^{1+\beta}$ [11] with $\beta = 0.07$ at $T = 0.32$ K. Due to the presence of surface accumulation states, conduction electrons experience scattering with random potential and the wire can be considered as in the disorder regime. Coulomb interactions related to charge redistribution between randomly positioned disorder potential wells with varying strength were shown to deplete the density of states at the Fermi level [12]. At higher temperatures, the differential resistance peak is smeared as seen from the grey and blue curves measured at 4 K and 300 K, respectively.

The differential resistance peak was further studied in several magnetic fields, as shown in figure 2(*a*). As would be expected, the electron–electron interaction is not strongly affected by the magnetic field and the overall shape of the curves is preserved. To quantify the observation, we swept the magnetic field and measured the differential resistance at several fixed bias voltages. The recorded R_d–B curves are depicted in figure 2(*b*) for perpendicular fields ramped back and forth between -50 kGs and $+50$ kGs at $T \approx 0.35$ K. The differential resistance shows aperiodic oscillation, which is symmetric in field and persists all the way to high magnetic fields. The non-self averaging fluctuations are reproducible and cannot be overlooked as noise.

In the weak disorder regime, one can associate the MR fluctuations with impurity scattering, which enhances [13] the electron–electron interaction described above. A sweeping magnetic field may be viewed as to change the impurity configurations, giving rise to the MR fluctuations. In the mesoscopic regime the sample size is smaller than or comparable to the phase breaking length and a zero-bias universal conductance fluctuation (UCF) amplitude of the order of e^2/h is expected [14, 15]. Since the contact resistance does not contribute to the MR, it is subtracted from the measured R_d and we obtained a conductance fluctuation amplitude of about $0.15e^2/h$ (figure 3(*a*)). An estimate for the phase breaking length L_φ can be obtained using the scaling law of the form $\delta G = (L/L_\varphi)^{-3/2}$ proposed by Skocpol [16] and discussed again by Beenakker and van Houten [17], where L is the length of the wire between the electrodes. In our case, L is about 120 nm, and using the observed amplitude of conductance fluctuations, the phase breaking length is estimated to be of the order of 34 nm. Phase coherence length in InN nanowires has already been addressed meticulously as a function of both temperature and wire size [18] and our data are consistent with the reported results.
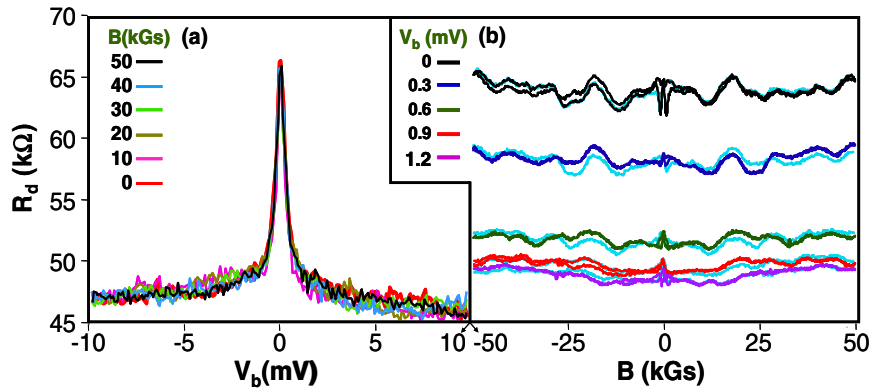
Figure 2. (*a*) Differential resistance as a function of bias voltage in various perpendicular magnetic fields. (*b*) Magnetic field dependence of differential resistance measured at various bias voltages. The vertical coordinate is the same as in (*a*). In (*b*) curves from the top are plotted for $V_b = 0$ to 1.2 mV in steps of 0.3 mV and are not shifted. The magnetic field was ramped from -50 kGs to $+50$ kGs and to -50 kGs. To show reproducibility, cyan curves taken from another set of measurements are displayed on the same plot. All data shown in (*a*) and (*b*) were taken at $T \approx 350$ mK using lock-in technique with 1.7 Hz, $19.3\,\mu$V excitation voltage. (Colour online.)
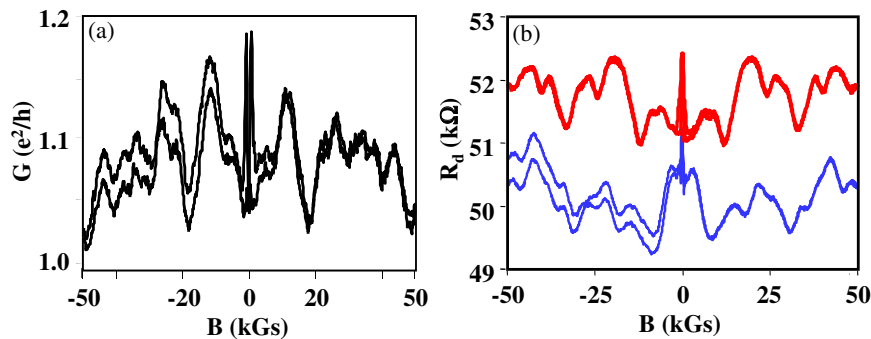
Figure 3. (*a*) Conductance fluctuations normalized to e^2/h obtained from $V_b = 0$ trace in figure 2(*b*). (*b*) MR fluctuations measured at $V_b = +0.59$ mV (red) and -0.58 mV (blue) in magnetic fields ramping back and forth between -50 kGs and $+50$ kGs. (Colour online.)

In spite of the smallness of δG, we note that the MR fluctuation pattern is symmetric with respect to sign reversal of the magnetic field originating from Onsager's relations of reversibility [18, 19]. The bias voltage dependence of the MR fluctuations is less explored. As shown in figure 2(*b*), upon increasing bias voltage three features are observed: (1) the amplitude of MR fluctuations decreases, (2) the MR patterns change with bias voltage, but certain correlation exists and (3) the symmetry survives even at high bias voltages. Increasing the bias voltage would increase the momentum of electrons participating in the transport [20], surmounting the counteracting electron-impurity scattering, leading to a monotonic decrease in the MR fluctuations. However, since the impurity configuration is not to be changed by the biasing electric field, the MR patterns should retain. In reality, the bias voltage causes a minute rearrangement of the charge impurity configuration and gives rise to progression of the MR patterns.

This bias-driven rearrangement of impurities is reversible and is confirmed by repeated measurements, shown as cyan traces in figure 2(*b*). Identical patterns of the MR fluctuations upon current reversal are suggested by Onsager's relations. However, as highlighted in figure 3(*b*), the patterns are not identical even with the same magnitude of current (i.e. bias voltage), implying that time reversal symmetry is not preserved. We find that the symmetry of the MR patterns with

magnetic field reversal is much more robust in comparison with the bias voltage reversal.

This interesting discrepancy has been observed in a few diffuse metallic systems where MR is symmetric in magnetic field and the asymmetry in electric field was attributed to short phase breaking lengths and the absence of an inversion symmetry centre [21]. As clearly seen in the amplitude of our conductance fluctuations, we are in the mesoscopic limit and the observed UCF asymmetry in bias reversal can be understood in the light of Thouless energy. Thouless energy is a measure of the diffusion broadening of eigen states, defined as $E_T \approx \hbar/t_T \approx \hbar D/L^2$, where t_T is the diffusion time for travelling through a sample of length L or Thouless time. In our case E_T is about $16\,\mu$eV using $D = 3.4 \times 10^{-4}$ m^2 s^{-1} [22] and $L = 120$ nm. It was proposed that applied bias voltages greater than E_T/e result in an arbitrary change in phase information [23] and this explains the observed MR asymmetry and breakdown of time reversal symmetry at bias voltage $V_b = 0.59$ mV shown in figure 3(*b*).

Experimental study of this evolution requires more dense data sets, which would be a subject for our future work.

The effect of magnetic field orientation on the magneto-oscillation was also studied. In figure 4(*a*) we can clearly see that the resistance fluctuations are hazier for the magnetic field parallel to the wire direction compared with that for the
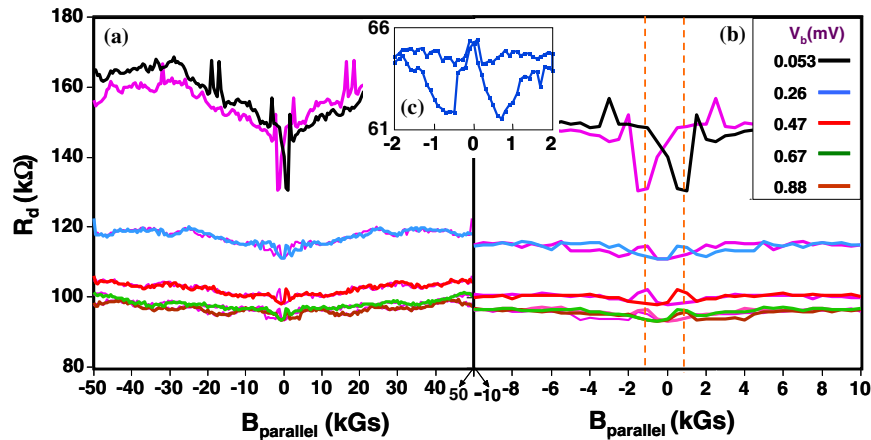
Figure 4. (*a*) Differential resistance measured at various bias voltages in parallel magnetic fields ramping back and forth between −50 kGs and +50 kGs. (*b*) A blowup of the low field region showing TMR structures and the orange dotted lines corresponding to coercivity field of the Ni electrodes. (*c*) Measured low field MR signatures from a different device, clearly identifying the switching field of Ni electrodes. The X and Y labels are identical to that of main panels. The bias voltages for each curve (from top) are 0.053(black), 0.26(blue), 0.47(red), 0.67(green) and 0.88 mV (brown). The magenta traces are the data points for reverse magnetic field sweeps. Data were taken at $T = 190\,\mu$K and excitation voltage of 96 μV. (Colour online.)

perpendicular field shown in figure 2(*b*). In both perpendicular and parallel fields, there is a dip in the differential resistance near 1 kGs, and similar switching fields were reported for the case of pure nickel nano-junctions [24, 25]. Also note these dips are prominent only for zero-bias resistance and are smeared in high bias regions in both parallel and perpendicular fields. These low field MR and hysteresis signatures can be understood in the light of TMR which originated from the difference in the spin density of states in the two ferromagnetic electrodes in the antiparallel and parallel magnetization configurations. At high bias voltages, typical TMR structures with peak in R_d in antiparallel magnetization are observed. However, at small bias voltages (see curve for 53 μV), we find a reversed TMR structure. Similar switching from inverse TMR at low bias to normal TMR at high bias has also been observed in three different systems. Firstly, this phenomenon is reported in a Ni/NiO/Co system [26] where they argued that there is a finite probability of spin polarization inversion inside the oxide layer due to disorder driven statistical variations. Secondly, Tan *et al* [27] have also reported very similar switching in superlattices of Co–Fe nanoparticles and highlighted the importance of electron–electron Coulomb interactions prevalent at low bias and low temperatures. Thirdly, the same behaviour reported in a Ni/InAs/Ni Coulomb blockade system [28] was attributed to spin filtering effects from the majority and minority bands of the ferromagnetic leads. While the above examples are of different systems, the underlying physics of the observed switching behaviour remains the same, namely, the Coulomb blockade effects. However, the precise consensus of the role of electron–electron Coulomb interactions on the sign of TMR is not available to date. We propose an intuitive explanation of the observed signatures to serve as pointers for future efforts. Recall that in figure 2(*a*), the high R_d value in the low bias region is attributed to the strong electron–electron interactions, resulting in the Coulomb blockade feature. Undoubtedly, there is a clear relationship between the observed sign of TMR and

the electron–electron interaction. The low energy electron–electron scattering events involving exchange interactions lead to pronounced spin flips, and this has been theoretically established using the quantum scattering approach in quantum dots [29] and generalized to metals [30]. However, at high bias the R_d is smaller and there is no significant contribution from the electron–electron interactions (due to smaller scattering cross-section [28]) and thus the normal TMR is restored. The evolution from low field TMR structure to high field MR fluctuations thus indicates a crossover from the spin-dependent transport to scattering mediated transport at the surface.

In summary, we present MR signatures in both parallel and perpendicular magnetic field configurations for a disorder InN nanowire. Interesting symmetry effects upon reversal of magnetic and electric fields on the electron transport are discussed in the regime where impurity scattering plays a significant role, observed in the form of magneto-fingerprints. The use of ferromagnetic electrodes gives additional structures at low magnetic fields, originating from typical TMR effects.

Acknowledgments

References

[1] Li Y, Qian F, Xiang J and Lieber C M 2006 *Mater. Today* **9** 18
[2] Guo Q X, Nishio M, Ogawa H, Wakahara A and Yoshida A 1998 *Phys. Rev.* B **58** 15304
[3] Wu J, Walukiewicz W, Yu K M, Ager J W III, Haller E E, Lu H, Schaff W J, Saito Y and Nanishi Y 2002 *Appl. Phys. Lett.* **80** 3967

[4] Tansley T L and Foley C P 1986 *J. Appl. Phys.* **59** 3241

[5] Al'tshuler B L, Kravtsov V E and Lerner I V 1986 *JETP Lett.* **43** 441

[6] Hu M S, Wang W M, Chen T T, Hong L S, Chen C W, Chen C C, Chen Y F, Chen K H and Chen L C 2006 *Adv. Funct. Mater.* **16** 537

[7] Mahboob I, Veal T D, McConville C F, Lu H and Schaff W J 2004 *Phys. Rev. Lett.* **92** 036804

[8] Mahboob I, Veal T D, Piper L F J, McConville C F , Lu H, Schaff W J, Furthmuller J and Bechstedt F 2004 *Phys. Rev.* B **69** 201307

[9] Chang C Y, Chi G C, Wang W M, Chen L C, Chen K H, Ren F and Pearton J 2005 *Appl. Phys. Lett.* **87** 093112

[10] Ping Sheng 1980 *Phys. Rev.* B **21** 2180
Lin Y H, Chiu S P and Lin J J 2008 *Nanotechnology* **19** 365201

[11] Fogler M M, Malinin S V and Nattermann T 2006 *Phys. Rev. Lett.* **97** 096601

[12] Efros A L and Shklovskii B I 1975 *J. Phys. C: Solid State Phys.* **8** L49
Beloborodov S *et al* 2007 *Rev. Mod. Phys.* **79** 469

[13] Eiler W 1984 *J. Low Temp. Phys.* **56** 481

[14] Lee P A and Stone A D 1985 *Phys. Rev. Lett.* **55** 1622

[15] Beenakker C W and van Houten H 1988 *Phys. Rev.* B **37** 6544

[16] Skocpol W J 1987 *Phys. Scr.* **T19** 95

[17] Beenakker C W J and van Houton H 1991 *Solid State Phys.* **44** 1

[18] Blomers Ch, Schapers Th, Richter T, Calarco R, Luth H and Marso M 2008 *Appl. Phys. Lett.* **92** 132101

Blomers Ch, Schapers Th, Richter T, Calarco R, Luth H and Marso M 2008 *Phys. Rev.* B **77** 201301(R)

[19] Onsager 1931 *Phys. Rev.* **38** 2265
Casimir H B G 1945 *Rev. Mod. Phys.* **17** 343

[20] Anaya A, Bowman M B, Korotkov A L and Davidovic D 2005 *Phy. Rev.* B **72** 035452

[21] Kaplan S B 1988 *Phys. Rev.* B **38** 7558

[22] Jia Z W, Shen W Z, Ogawa H and Guo Q X 2004 *Appl. Phys. Lett.* **89** 232107

[23] Murek U, Schafer R and Langheinrich W 1993 *Phys. Rev. Lett.* **70** 841
Holweg P A M, Kokkedee J A, Caro J, Verbruggen A H, Radelaar S, Jansen A G M and Wyder P 1991 *Phys. Rev. Lett.* **67** 2549

[24] Yang C S, Zhang C, Redepenning J and Doudi B 2004 *Appl. Phys. Lett.* **84** 2865

[25] Viret M *et al* 2002 *Phys. Rev.* B **66** 220401

[26] Tsymbal E Y, Sokolov A, Sabirianov I F and Doudin B 2003 *Phys. Rev. Lett.* **90** 186602

[27] Tan R P, Carrey J, Desvaux C, Grisolia J, Renaud P, Chaudret B and Respaud M 2007 *Phys. Rev. Lett.* **99** 176805

[28] Hamaya K, Kitabatake M, Jung M, Kawamura M, Ishida S, Taniyama T, Hirakawa K, Arakawa Y and Michida T 2008 *Appl. Phys. Lett.* **93** 222107

[29] Castelano L K, Hai G Q and Lee M T 2007 *Phys. Status Solidi* c **4** 466

[30] Solleder B, Lemell C, Tokesi K, Hatcher N and Burgdorfer J 2007 *Phys. Rev.* B **76** 075115